Contribution of zeolite-seeded experiments to the understanding of glass resumption of alteration

M. Fournier, S. Gin, P. Frugier, S. Depierre

npj | Materials Degradation

www.nature.com/npjmatdeg

ARTICLE OPEN

Contribution of zeolite-seeded experiments to the understanding of resumption of glass alteration

Maxime Fournier[1], Stéphane Gin[1], Pierre Frugier[1] and Sara Mercado-Depierre[2]

Understanding the origin and the consequences of glass alteration regimes is necessary for the prediction of nuclear glass durability. The so-called "stage 3" or "resumption of alteration regime" of glasses used to sequester nuclear waste by vitrification, is characterized by a sudden acceleration of glass alteration rate arising from the precipitation of secondary minerals, mainly zeolites. To study this process, a promising approach is developed, based on seeding by synthesized zeolite seeds. This study quantitatively links the alteration of a six-oxide reference borosilicate glass (ISG) and the precipitation of zeolites that affects concentrations of key species—in particular aluminum—and thus the glass dissolution rate. The characterization of stage 3—easier at alkaline pH—can now be extended to pH conditions more representative of those found in a geological repository thanks to seeding that reduces, or even eliminates, the latency period preceding a resumption of glass alteration. The resumption occurrence and glass dissolution rate are related with temperature and pH. This study shows that the detrimental effect of zeolite precipitation decreases with decreasing pH and temperature, until it is no longer detectable at a pH around 9 imposed by the dissolution of the ISG glass. Even for both high temperature and high pH, the resumption rate is lower than the initial alteration rate, which remains the fastest kinetic regime.

npj Materials Degradation (2017)1:17 ; doi:10.1038/s41529-017-0018-x

INTRODUCTION

Like the United Kingdom, Japan, Russia and India, France has chosen to reprocess spent nuclear fuel. Ultimate waste arising from this recycling process—consisting of fission products and minor actinides—are confined by vitrification. The reference solution for the management of these waste packages over geological time scales is their storage in a deep, low-permeability and stable geological formation.

In contact with water, the vitrified product of waste, usually called "nuclear glass", undergoes both dissolution and irreversible transformation into more stable phases; the rate of this transformation strongly depends on geochemical conditions. Formation of a passivating layer (also called "gel") causes the reduction of the initial alteration rate r_0—due to the hydrolysis of the vitreous network by nucleophilic substitution of hydroxide ions—until the persistence of a residual rate. For a glass, this gel can exhibit a great variability in composition—and thus in properties—depending on the environmental parameters, in particular pH, temperature and solution composition. Gel stability and its passivation properties allow—under the most favorable conditions—a glass package lifetime of hundreds of thousands to millions of years. However, a resumption of alteration (RA, also called "stage 3" in the literature)—i.e., a sudden acceleration of the glass alteration rate—can occur.[1,2] Resumptions of alteration have been observed in specific experimental conditions, particularly in alkaline environments—as a consequence of the dissolution of alkali-rich glasses or cement—at relatively high temperatures (typically above 90 °C) and high glass-surface-area-to-solution-volume (*S/V*) ratios.[3–7] This phenomenon is associated with the precipitation of alumino–silicate minerals, mainly from the zeolite family.[8–10]

Understanding the origin of a RA and evaluating its consequences are major issues to predict nuclear glass long-term behavior. Under high pH and temperature conditions, it is established that zeolite precipitation maintains glass alteration at a high rate. The question then arises of whether this could also be the case under moderate temperature and pH conditions.[11] Answering this question is made difficult by the potentially very long latency period preceding RA—corresponding to the time taken to produce stable nuclei—and the many coupled processes involved at the microscale or nanoscale depending on the glass composition or the leaching conditions. Reducing the latency period could be achieved following a new approach: seeding, i.e., the addition of zeolite seeds promoting the formation of these minerals.

Seed crystal addition during zeolite synthesis is a common industrial practice to significantly accelerate the crystallization rate of these minerals,[12,13] thanks to the reduction or elimination of the latency period.[14] Seed-assisted synthesis was initially kept for the synthesis of zeolites having the same crystalline structure as the seeds. Later, seeding appeared as a good way to control the structure of the phases that crystallize[15–18] provided that the seeds—which then act as structure-directing agents—have structural similarities with the zeolites to be obtained.[19,20]

A mechanism explaining the effect of seeds was proposed by Xie, et al.[21] At the beginning of the reaction, the partial dissolution of seeds[17,18,21] releases soluble alumino–siliceous species and crystalline particles into solution. During the growth of new crystals on the seed surface, these particles act as structure-directing agents,[16] leading to the development of viable crystals. The seed growth—very predominant compared to new nucleation[18,21,22]—is controlled by the surface area developed

[1]CEA, DEN, DE2D, SEVT, F-30207 Bagnols sur Cèze, France and [2]CRITT Matériaux Alsace, F-67305 Schiltigheim, France
Correspondence: Maxime Fournier (maxime.fournier@cea.fr)

Received: 22 March 2017 Revised: 29 August 2017 Accepted: 6 September 2017
Published online: 13 November 2017

Table 1. Alteration rates in unseeded tests

Test reference	T (°C)	Δt_P (days)	r_P (g m^{-2} d^{-1})	t_{RA} (days)	r_{RA} (g m^{-2} d^{-1}) [R^2]
US-1770-11.3	90	Not observed	–	1–2	3.3 [0.98]
US-1770-11.0	90	9 (6–15)	1.3×10^{-2}	15–21	1.9 [0.97]
US-1770-10.7	90	23 (6–29)	8.7×10^{-3}	29–40	7.5×10^{-1} [0.76]
US-1770-10.4	90	83 (3–86)	2.5×10^{-3}	86–119	5.6×10^{-2} [0.97]
US-1770-10.1	90	>243 (86–end)	$\approx 2 \times 10^{-3}$	Not observed	–
US-1770-F	90	>210 (119–end)	3.2×10^{-3}	Not observed	–
US-70-11.3	90	Not observed	–	0–5	≈8
US-70-11.0	90	≈8 (5–13)	$\approx 7 \times 10^{-1}$	13–24	≈8
US-70-10.7	90	≈11 (13–24)	$\approx 2 \times 10^{-1}$	24–40	2.1 [0.98]
us-1770-13.1	30	197 (110–307)	4.6×10^{-3}	250–307	9.8×10^{-3} [0.93]
us-1770-12.7	30	>590 (110–end)	6.2×10^{-4}	Not observed	–
us-1770-12.3	30	>590 (110–end)	9.4×10^{-5}	Not observed	

Duration (Δt_P) and glass alteration rate (r_P) plateauing during the latency period preceding the resumption of alteration. Onset time (interval t_{RA} between the last sample before the resumption and the first one during the resumption) and rate (r_{RA}) of the resumption of alteration for unseeded tests. r_{RA} is determined by linear regression: coefficient of determination R^2 shown in square brackets indicates that this assumption is reasonable; furthermore, the maximum rate calculated by the moving average does not exceed $2.5 \times r_{RA}$

by the crystals present in the reactor, which determines how quickly the system crystallizes and its final crystallinity.[12,15,23]

In the literature, the effect of the initial presence of zeolitic secondary phases on the glass alteration behavior is shown by leaching tests of pre-altered monoliths alone in solution[24,25] or in contact with pristine glass.[8] Such tests emphasize an exacerbated alteration of the glass in the presence of secondary phases—zeolites in particular—formed during the glass pre-alteration. However, the initial presence of zeolites is not the only factor that can explain the increase of the dissolution rate observed in these experiments: an increase of pH due to the partial dissolution of secondary phases[25]—which contributes to the acceleration of the glass alteration rate—is also shown.

Moreover, the literature provides a few examples of nuclear glass leaching tests in the presence of natural zeolite seeds.[26–28] The results of these studies are contrasted, showing the presence[27] or absence[26,28] of an effect of seeding on glass alteration, but suggest the need for a sufficient structural similarity between the seeds used and the zeolites that may form during glass alteration to ensure the success of seeding. This point will be examined in the following.

The present study highlights the links between RA and precipitation of zeolites (and, to some extent, of calcium silicate hydrates). The aim is to quantify the degree of alteration of glass related to the mechanisms of formation of these phases. Seeding, pH, temperature and *S/V* ratio are used as variables. The use of buffered pH ensures better interpretation of the results and the determination of reliable parameters to support future modeling work. The efficiency of seeding is proved, and the consequences of zeolite precipitation on glass durability for a wide range of pH and temperature values are discussed.

RESULTS

Unseeded leaching tests

Alteration rate measurements. Unseeded tests are presented as references, which are then compared to seeded experiments in the following. Some of these unseeded experiments were previously described:[29] a brief summary of the results obtained is given below, and alteration rates—normalized as explained in Methods section—are given in Table 1. Other tests were conducted to explore lower pH or study the influence of *S/V* ratio and temperature.

At 90 °C and $S/V = 1770$ m^{-1} (Fig. 1), the RA occurs after a latency period during which the alteration rate plateaus at a low value ("plateau rate" r_p) and whose duration diminishes as the pH increases. A RA is observed between pH = 10.4 and 11.3 but not at free pH (approximately 9). Its occurrence at pH = 10.1 is discussed in the following paragraphs. The altered glass fraction (AGf) during the latency period is higher for the free pH experiment than that achieved during the latency period of the higher pH tests. This is consistent with the fact that, at high *S/V* ratio, processes leading to the boron release[30,31] become slower with increasing pH.[32]

Alteration rates measured during the latency period (r_P) and the r_{RA} are reported in Table 1. r_{RA} is defined as the rate reached since the inflection point following the latency period and until the total alteration of the glass sample is about to be reached (or the end of the experimental period). Note that this simple criterion refers to a process whose reality is probably the convolution of several limiting mechanisms and therefore sensitive to other parameters in addition to pH, such as zeolite surface area or solution composition. The time at which the RA occurs and the corresponding rate are qualitatively correlated with pH.

As expected, at the beginning of the experiments, the higher the pH is, the higher is the aluminum concentration in solution. The further decrease in the aluminum concentration is likely caused by the nucleation of aluminous phases. The decrease in the aluminum concentration starts before the increase in the boron concentration: this is likely because aluminous phases precipitation first consumes the dissolved aluminum available in solution, before the glass dissolution provides more aluminum. In this respect, it should be noted that the beginning of the decrease in the aluminum concentration is a precursor of the RA, and thus a good indication of its imminence. As an example, the case of test US-1770-10.1 is particularly interesting: although boron concentration increases at nearly constant rate—consistent with a RA—it does not show a "slope break" typical of the resumption beginning, but the aluminum concentration is decreasing continuously.

When decreasing, aluminum concentration achieves a minimum, which can be followed in some experiments (e.g., US-1770-11.3), by a slight new increase after glass has completely altered: this phenomenon suggests a change in the gel or secondary phase assemblage. An evolution in the zeolite composition is a possible explanation although this has not been proved.

In the experiment at $pH_{90\,°C} = 10.4$ (US-1770-10.4; pink squares on Fig. 1), a glass alteration rate increase is observed after

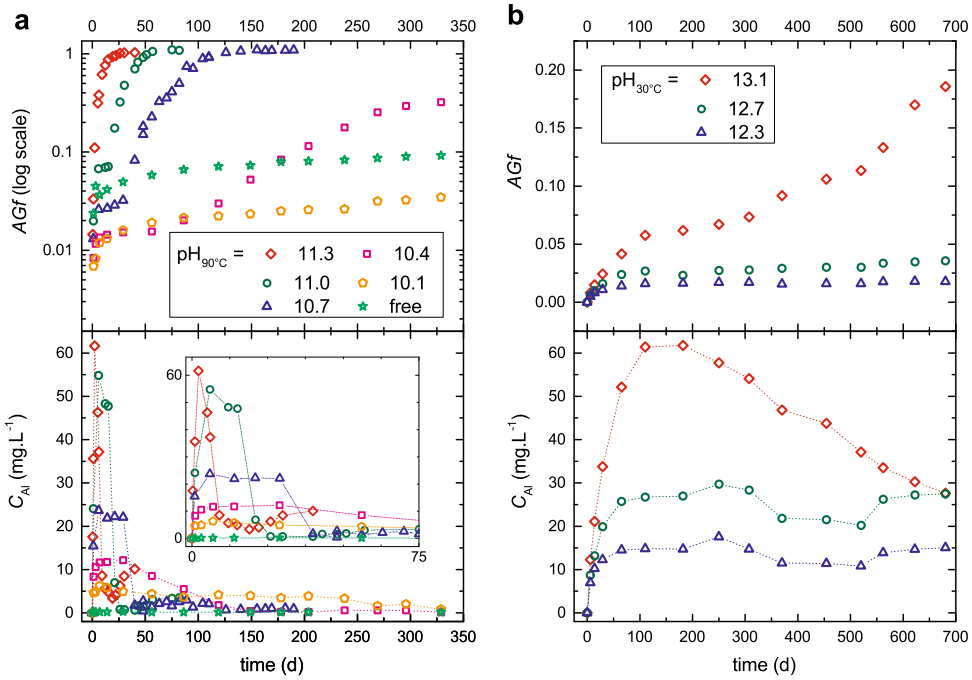

Fig. 1 Unseeded leaching tests results: at **a** 90 °C (US-1770 test series) and **b** 30 °C (us-1770 test series) with an *S/V* ratio of 1770 m^{-1}. Graphs show the evolution of the altered glass fraction AGf (top) and the aluminum concentration (bottom and insert)

100 days, 50 days after the aluminum concentration starts to decrease. Moreover, during the resumption period and after the aluminum activity becomes minimal, the resumption rate is inflected ($t > 250$ days): the alteration rate is approximately 2 orders of magnitude lower than the initial rate measured by Inagaki, et al.[33] The observation of such a rate drop in a pH-buffered experiment is new and could be due to a zeolite growth limited by (i) the lack of aluminum available in the system or (ii) the persistence of a passivating gel at this pH value.

Leaching tests with an *S/V* ratio of 70 m^{-1} and a temperature of 90 °C (Supplementary Fig. 1) confirm the observations made at *S/V* = 1170 m^{-1} about the role of pH on the time at which the resumption is triggered and its corresponding rate: the higher the pH, the earlier the resumption appears with a higher rate. Although there were too few solution samplings during these tests to ensure precise rate calculations, estimated values are given in Table 1. The effect of the *S/V* ratio on resumptions of alteration will be discussed later, it should be noted in this regard that at this *S/V* ratio of 70 m^{-1}—and with an alteration solution enriched with silica (see Methods section)—resumption rates are somewhat higher and latency periods are shorter than at *S/V* = 1770 m^{-1}.

For tests conducted at 30 °C and alkalinities identical to those used at 90 °C (i.e., same pOH), the alteration rate stabilizes after 100 days at the two lowest pH values (Fig. 1b). Only the experiment at the highest pH shows a RA, resulting in a constant decrease in the aluminum concentration starting from day 250 and a marked increase of AGf from Day 400. During the resumption, the alteration rate is four times greater than that measured during the latency period. One can wonder whether aluminum concentration will continue to decrease with time, while the alteration rate continues to increase.

Secondary phases identification. Secondary phases precipitated when alteration resumes—at 90 °C for both *S/V* ratios—were identified by X-ray diffraction (XRD) assisted by Scanning electron microscopy (SEM) (see also Fournier, et al.[29]). These phases are a mixture of zeolites Na-P2, zeolites Na-P1, and calcium silicate hydrates (C–S–H; note that the possibility that these phases incorporate a small amount of aluminum is not excluded), sometimes with a small amount of analcime (Fig. 2a and Supplementary Fig. 4). Overall, zeolites P2 predominate at $pH_{90\,°C} > 10.7$ and zeolites P1 at $10.4 \leq pH_{90\,°C} \leq 10.7$. Stoichiometries of zeolites formed in test series US-1770 were evaluated by SEM/EDS, giving a Na/Al ratio ≈ 1 and a Si/Al ratio varying with pH: 2.9 at $pH_{90\,°C} = 10.7$; 2.4 at $pH_{90\,°C} = 11$ and 2.1 at $pH_{90\,°C} = 11.3$. This decrease in the Si/Al ratio with increasing pH is consistent with the literature.[3,34,35]

SEM shows that C–S–H cover the surface of glass grains, and their presence is confirmed by the broad reflection with highest intensity at ≈29° 2θ on XRD patterns.[36] During leaching tests in alkaline media, glass grains gradually hollow out (Supplementary Fig. 2). The "outer shell" of the grain remains, probably cemented by C–S–H. Pristine glass is separated from this shell by one or more amorphous layers, mainly composed of silicon, sodium and zirconium non-precipitated in the secondary phases.

Once the glass is completely altered—and while the pH remains constant—analcime precipitates slowly, probably by conversion of metastable zeolites P,[37] as seen in Fig. 2b. Moreover, the peaks corresponding to the zeolite P shift substantially towards larger angle, indicating a decrease in the zeolite lattice parameter; this contraction reflects an impoverishment of the lattice into one of its components, whose nature remains indeterminate.

For test us-1770-13.1—performed at 30 °C—in which a RA is seen, SEM and XRD (not shown here) failed to identify zeolite crystals, probably because the amount precipitated is too small. Only C–S–H are observed—these phases are also known to participate in the resumption phenomenon.[10,38]

Characterizations of synthetized seeds

The results shown in the previous section indicate that the nature of precipitated secondary phases varies little during the ISG (international simple glass) glass RA at 90 °C between $pH_{90\,°C} =$ 10.4 and 11.3. Under these conditions, most zeolites are those of the zeolites P family. These zeolites have been synthesized since the late 1950s;[39] in particular, zeolite Na-P2 is considered to be the synthesic zeolite similar to gobbinsite,[40] whose crystal structure

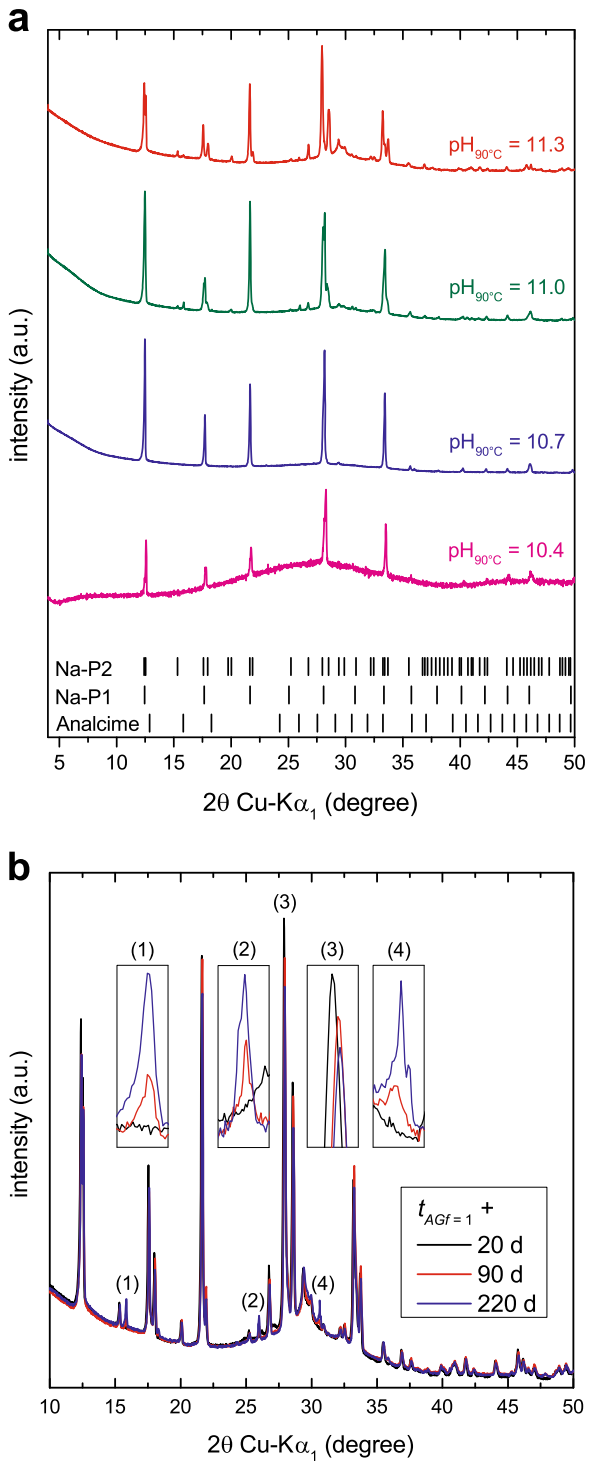

Fig. 2 Secondary phases identification. **a** X-ray diffraction patterns for tests performed at 90 °C with an *S/V* ratio of 1770 m^{-1} (test series US-1770). The identified phases are zeolite Na-P2 (JCPDS 80-0700), zeolite Na-P1 (JCPDS 71-0962) and analcime (JCPDS 76-0904). **b** X-ray diffraction patterns of crystalline phases formed 20, 90 and 220 days after achieving complete glass alteration ($t_{AGf=1}$) at 90 °C and $S/V = 1770\ m^{-1}$. Peaks 1, 2, and 4 on which are performed the magnifications correspond to the major peaks of analcime: it becomes more intense as the peaks of the zeolites P become less intense (peak 3)

determination[41] confirms its affiliation in the GIS group with an orthorhombic cell (*Pnma*). This zeolite was synthesized—according to the protocol presented in Methods section—to be used as seeds in the following and characterized.

The morphology of synthesized seeds (Supplementary Fig. 3a) is significantly different from that of neoformed zeolites (Supplementary Fig. 3b), but their crystalline structure is identical (Supplementary Fig. 3c). IR spectroscopy (Supplementary Fig. 3d) shows strong vibration bands attributed to internal vibrations of tetrahedrons TO_4.[42] The IR spectrum corresponds to that expected for a synthetic Na-P zeolite.[43,44]

The outer surface of these almost spherical seeds was evaluated by laser diffraction (Supplementary Fig. 3.e): particle size distribution shows (i) a bimodal distribution with maxima at 7 and 18 µm and (ii) the numbers of particles with a size less than 3 µm or greater than 100 µm are negligible. The geometric specific surface area (Eq. 1) resulting from this distribution is $S_z = 0.25\ m^2\ g^{-1}$ ($S_{z,\ BET} = 23\ m^2\ g^{-1}$). It will be shown in the following section that zeolite growth occurs on the seed outer surface, which is why the geometric surface area of the seeds is used as representative of their "reactive" surface area.

Thermogravimetric analysis (TGA) characterization (Supplementary Fig. 3f)—consistent with that expected for a Na-P synthetic zeolite[43,44]—shows two mass losses. The first 13 wt% loss in the 25–200 °C range is likely a loss of physisorbed water. The second 4 wt% loss in the 200–500 °C range is attributed to hydroxyl groups. The aluminum, sodium and silicon contents of the seeds were measured by ICP-OES after dissolution in acidic solution. Considering that 13% of the seed mass consists of adsorbed water, seed stoichiometry $Na_4Al_4Si_{6.8}O_{22.4}{\cdot}8\ H_2O$ is close to that obtained by Barrer and Munday[45] or Taylor and Roy.[46] Moreover, the Si/Al = 1.7 and Na/Al = 1 ratios are close to those of neoformed zeolites.

Seeded leaching tests

Alteration rate measurements. The tests discussed in this section are performed in the same experimental conditions as those for unseeded tests described previously, with a major difference: the glass powder is mixed with the zeolite seeds. The reactive surface area ratio between zeolites and glass (S_z/S) is 0.07 for S-1770 test series, 1.1 for s-1770 test series and 1.5 for s-70 test series. Note that the effect of the S_z/S ratio is also investigated for tests S-1770-10.1 and S-1770-F and presented later.

At 90 °C, remarks about unseeded tests remain valid in the presence of seeds for the two *S/V* ratios tested (test series S-1770 and S-70): the higher the pH, the earlier the resumption appears and the higher the rate (Fig. 3a and Supplementary Fig. 5). The alteration rates are higher in seeded tests (Table 2), except at free pH where no significant difference is evidenced (regardless of which S_z/S ratio used).

At 30 °C (Fig. 3b, s-1770 test series), although the S_z/S ratio is 17 times higher than in comparable experiments at 90 °C, no RA—in its original definition—seems to be visible. However, the alteration rate is significantly higher than in the corresponding unseeded test shown in Fig. 1b. In addition, the aluminum concentration is maintained at a lower value than in the unseeded tests and starts to decrease at the two higher pH values. These are two pieces of evidence that the zeolite precipitation rate in unseeded experiments could be limited by the zeolite surface area available at that time. As a consequence, alteration rates r_{RA} in unseeded experiments (Table 1) are expected to increase with time with increasing zeolite surface area up to, at least, the r_S value of seeded experiments (Table 2).

As mentioned in the introduction, the seeded mineral nature affects the efficiency of the process. Here, the seed choice could be validated only over the pH range 10.4–11.3 at 90 °C because the zeolite precipitation in these tests is sufficiently rapid to allow their characterization.

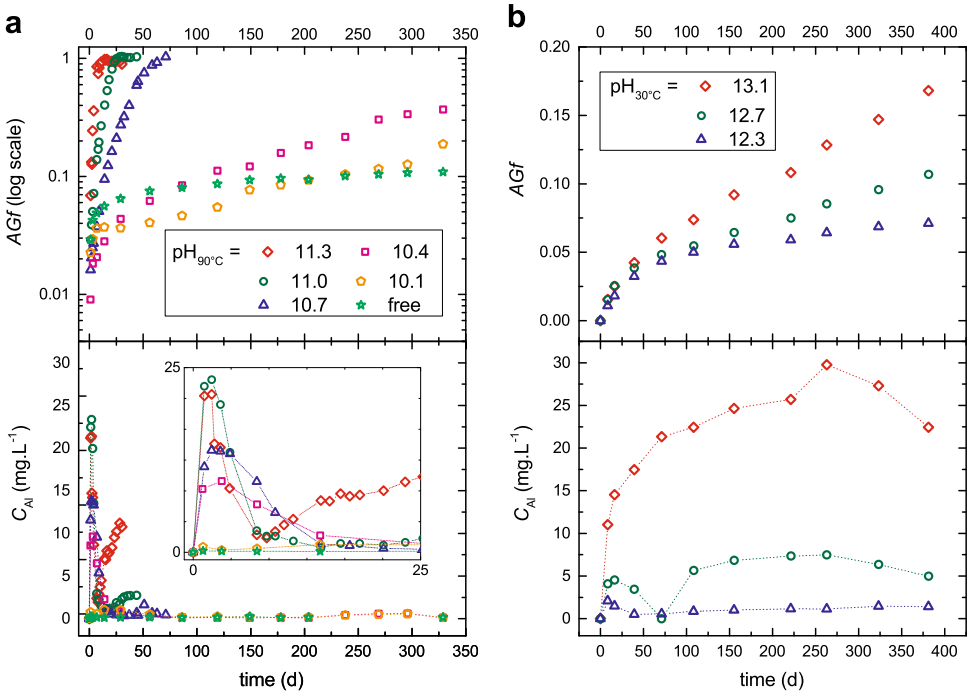

Fig. 3 Seeded leaching tests results: at **a** 90 °C (S-1770 test series) and **b** 30 °C (s-1770 test series) with an *S/V* ratio of 1770 m^{-1}. Graphs show the evolution of the altered glass fraction AGf and the aluminum concentration. Figure to compare with Fig. 1 for unseeded tests

Table 2. Alteration rate r_S measured in seeded tests during the time interval Δt_S

Test reference	*T* (°C)	Δt_S (days)	r_S (g m^{-2} d^{-1}) [R^2]
S-1770-11.3	90	1–11	5.5 [0.98]
S-1770-11.0	90	11–25	5.0 [0.90]
S-1770-10.7	90	32–63	1.5 [0.99]
			≈2.2 ($S_z/S = 0.16$)
			≈3.2 ($S_z/S = 0.28$)
			≈4.5 ($S_z/S = 1.1$)
S-1770-10.4	90	1–end	3.8×10^{-2} [0.95]
S-1770-10.1	90	86–296	1.3×10^{-2} [0.99]
S-1770-F	90	119–end	3.3×10^{-3} [0.93]
			4.5×10^{-3} [0.99] ($S_z/S = 1.1$)
S-70-11.3	90	1–7	≈18
S-70-11.0	90	1–16	6 [0.97]
S-70-10.7	90	23–50	4.2
s-1770-13.1	30	39–end	1.2×10^{-2} [1.00]
s-1770-12.7	30	39–end	6.6×10^{-3} [1.00]
s-1770-12.3	30	155–end	2.4×10^{-3} [0.98]

r_S is determined by linear regression (coefficient of determination R^2 is shown in square brackets). When not specified, $S_z/S = 0.07$. Table to compare with Table 1 for unseeded tests

Secondary phases identification. For tests conducted at 90 °C with $pH_{90\,°C}$ ranging between 10.4 and 11.3, secondary precipitated phases are identical with or without seeds: zeolites P (Na-P2 and Na-P1), small amounts of analcime, and C–S–H (e.g., Fig. 4a compares XRD patterns for S-1770-11.0 and US-1770-11.0). In the presence of seeds, diffraction peaks associated with zeolites P are more intense because the amount of zeolites produced by glass alteration is added to that of seeds. SEM indicates a clear growth of seeds (Fig. 4b), while the neoformed zeolites are smaller (Supplementary Fig. 6) than in unseeded tests. Zeolite growth on the seed surface is favored compared to the nucleation of new crystals.

For the tests conducted (i) at $pH_{90\,°C} < 10.4$ at 90 °C and (ii) at $T = 30$ °C, no neoformed zeolites could be identified beforehand in unseeded tests, so the seed choice in these conditions cannot be qualified a priori. Thus, at 90 °C and $pH_{90\,°C} = 10.1$, SEM imaging shows that the mineral formed on seed surfaces has a very different morphology from that of seeds (Fig. 5a); this mineral is identified as chabazite-Na by XRD (Fig. 5b). Thus, the growth of a sodium zeolite—different from the zeolite Na-P2—is favored in these experimental conditions. If seeding with zeolite Na-P2 remains effective to accelerate glass alteration kinetics, it is possible that this nature of seed is not the best adapted: a persisting latency period is observed (Fig. 3a, $t < 86$ days), and it could be hypothesized that a higher alteration rate would have been measured in the presence of chabazite seeds.

At 30 °C, glass alteration is sustained by a slow growth of the seeds, visible on SEM images (Supplementary Fig. 7). The amount of new crystals is too small to identify their nature by XRD.

Seeded leaching tests with various S_z/S ratios

Two tests (S-1770-10.7 and S-1770-free) were carried out with varying amounts of seeds to demonstrate the effect of the surface area accessible to the zeolite growth on the glass alteration. At alkaline pH—where a seed effect is demonstrated—the higher the seed surface, the faster the glass alteration (Fig. 6). The glass alteration rate evolution with the seed surface is not linear: it is expected that from a certain amount of seeds, seeding reaches a maximum effect, possibly limited by the achievement of a seed surface sufficient to mobilize all the elements available and necessary for the zeolites growth. Furthermore, as it will be shown in the following, note that at the pH imposed by the glass alteration itself (approximately 9), no effect of seeding is demonstrated, regardless of the amount of seeds added to the medium (Fig. 9c).

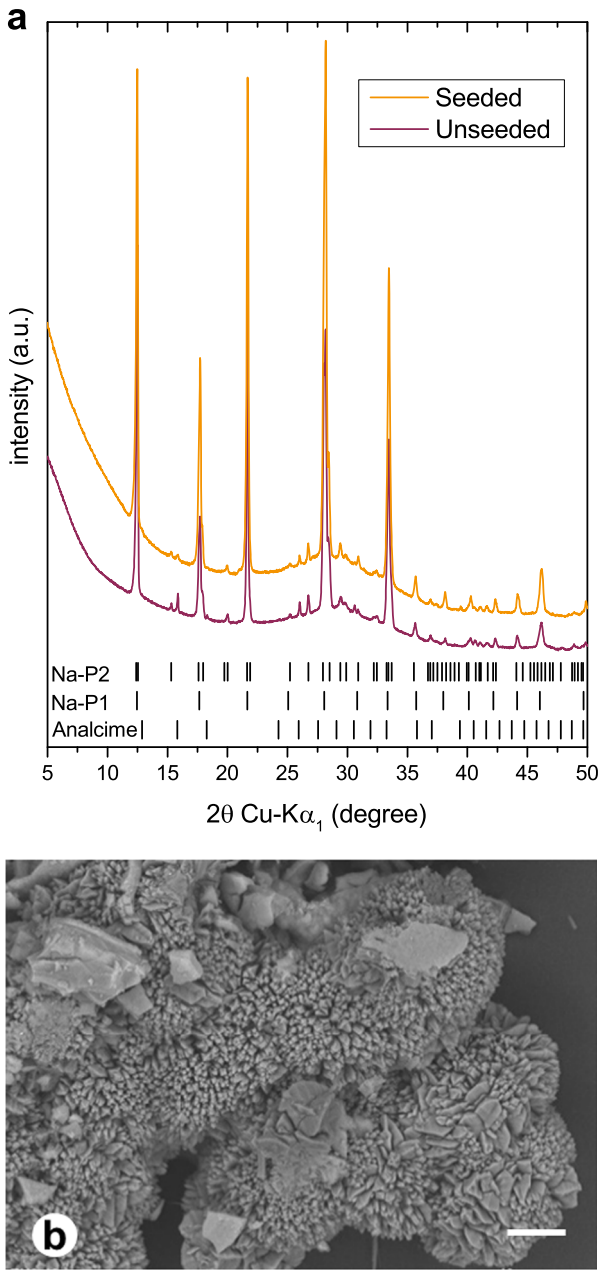

Fig. 4 Seeds growth at 90 °C, pH = 11. **a** X-ray diffraction patterns at the end of US-1770-11.0 and S-1770-11.0. The same secondary phases are identified with or without seeding: zeolite Na-P2 (JCPDS 80-0700), Na-P1 (JCPDS 71-0962), analcime (JCPDS 76-0904) and C–S–H. **b** Seed growth is clearly visible (picture to compare to Supplementary Fig. 3a)

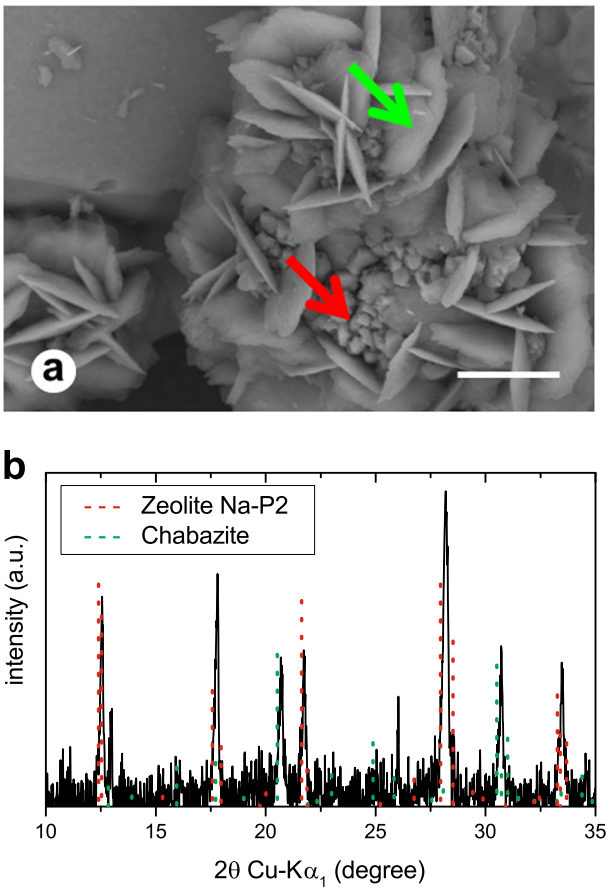

Fig. 5 Seeds growth at 90 °C, pH = 10.1. **a** At $pH_{90\,°C} = 10.1$, two crystals with very different morphologies are observed (seeds of Na-P2 zeolite indicated by the red arrow and neoformed crystals indicated by the green arrow). Scale bar represents 10 µm. **b** XRD identified Na-P2 zeolite (JCPDS 80-0700), introduced as seeds, which supports the growth of another zeolite: chabazite (JCPDS 34-0137). The background was subtracted for readability

DISCUSSION

This study highlights the efficiency of seeding: by the faster kinetics it induces, seeding allows the characterization of resumptions of alteration at pH and temperature values lower than those classically investigated in the time scale of the laboratory. Following paragraphs will deal with the effects of *S/V* ratio, seeding, pH, and temperature on the resumptions of alteration.

Effect of *S/V* ratio

The *S/V* ratio is usually considered as a parameter for designing leaching tests run in static conditions. Indeed, release rate of the elements from the glass, time and *S/V* ratio drive the solution composition, which in turn has a great effect on the glass dissolution rate. Therefore—though cautiously—*S/V* ratio is a parameter one can play with to investigate long-time-scale solution compositions. In experimental studies comparing glass alteration at various *S/V* ratios, the RA is observed earlier at high *S/V* ratios.[3–7]

In this study, it appears that the RA occurs earlier at the lower *S/V* ratio in both unseeded (Fig. 7 and Supplementary Fig. 8) and seeded tests. This would have been the contrary in deionized water but the tests carried out at a *S/V* of 70 m^{-1} were launched with a solution enriched in silica, thus favoring the precipitation of zeolites. As glass dissolves, silicon, aluminum and sodium concentrations increase and the solution may become saturated with respect to a zeolite. In the tests with $S/V = 70\ m^{-1}$, the initial silicon activity is higher due to the silica added to the leachant, and for a given pH, at $t = 0$, the sodium activity is equal regardless of the *S/V* ratio. Thus, a lower aluminum activity is sufficient to reach saturation with respect to zeolites in the experiments with an *S/V* ratio of 70 m^{-1}. Therefore, in the stability domain of zeolites, the supply of dissolved silica is particularly unfavorable for glass durability, while it is beneficial between pH = 7 and pH = 9.5,[10,47] as solutions remain undersaturated with respect to zeolites.

Note that at a low *S/V* ratio of 70 m^{-1}, the pH is maintained stable with only rare additions of small quantities of NaOH

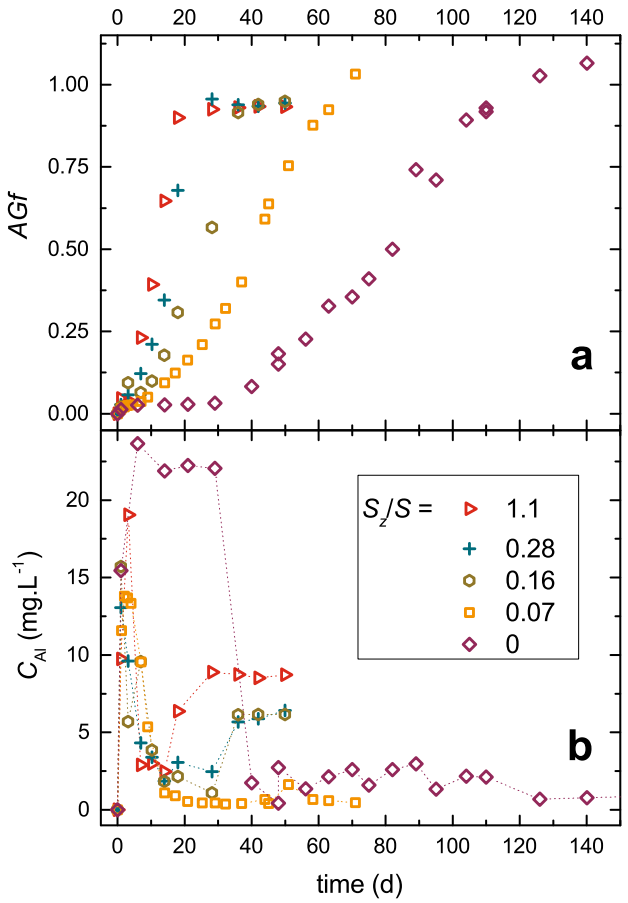

Fig. 6 Effect of seeding ratio. Seeded leaching tests at 90 °C, S/V = 1770 m^{-1}, $pH_{90\,°C}$ = 10.7 with various amounts of seeds

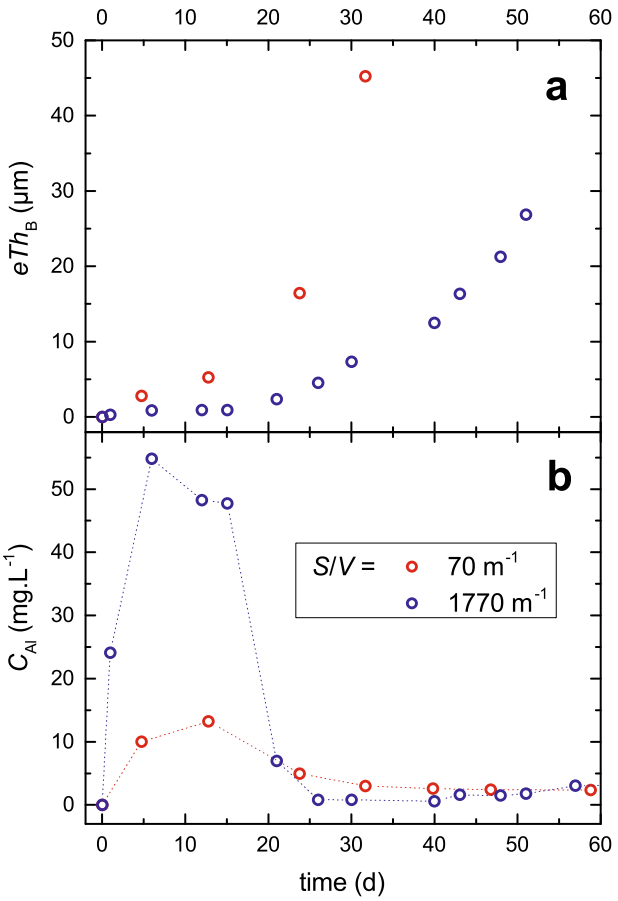

Fig. 7 Effect of S/V ratio. Comparison of **a** boron equivalent thicknesses of altered glass (eTh_B) and **b** aluminum concentrations in solution (C_{Al}) for tests conducted with S/V ratios of 1770 and 70 m^{-1} at 90 °C and $pH_{90\,°C}$ = 11.0

because of the small amount of glass with respect to the volume of solution to set this S/V ratio. Therefore, these tests allow the effect of the pH to be decorrelated from that of the additions of NaOH necessary to impose the pH: the results observed are mostly due to the effect of pH, and not sodium.

As a conclusion, mechanisms responsible for RA can be studied independently of the S/V ratio because the important parameter is the time required to achieve solution saturation with respect to zeolites.

Effect of seeding

Seeding as a tool to reduce latency period and accelerate kinetics. Seeding induces a significant decrease—even the total suppression—of the latency period taken to produce stable nuclei. For the most alkaline pH, glass is altered much more rapidly in the presence of seeds, and aluminum is consumed quickly.

As an example, the seeded and unseeded tests at 90 °C, $pH_{90\,°C}$ = 11 are compared in Fig. 8a: the maximum aluminum concentration is half in the presence of seeds. The silicon concentration increases during the resumption since it is in excess given the Si/Al ratios of the glass and the zeolites. It was shown elsewhere[48] that aluminum decreases the apparent solubility of silicon: more silicon is therefore released in solution because of the aluminum departure from the amorphous layers during the zeolite precipitation. The silicon concentration reached at the end of the experiment (once the glass is totally altered) is the same, which suggests that the same phase controls its activity in solution. The solubility of this phase would then be very far from that of amorphous silica—to which the solubility of a predominantly siliceous gel is generally assimilated. A lower temperature of 30 °C (Fig. 8b) does not change the nature of the phenomena observed at 90 °C but strongly slows down the kinetics.

There is evidence of an effect of the seed surface area, resulting in a higher rate of glass alteration when increasing the amount of seeds. This effect is not linear: a threshold—upper which the glass dissolution rate no increases whatever the amount of seeds—seems to be quickly reachable, but its existence has not been proved. Even with the highest S_z/S ratio, the resumption rate remains lower than the initial dissolution rate by a factor of 6: this could be due to a kinetic limitation of zeolite growth or to a passivating effect of the gel layer; this effect would be less strong than that encountered at less alkaline pH. However, the effect of the seed surface area on the duration of the latency period seems very limited.

Seeding as a tool to explore lower pH and temperatures, and to measure long-term alteration rates. Thanks to the reduction of the latency period, seeding allows the quantification of the effects of a possible precipitation of zeolites on borosilicate glasses in new pH ranges. This provides new perspectives that can address important issues when studying the behavior of glasses under representative conditions of geological storage in neutral or slightly basic pH conditions or when trying to unify laboratory approaches and field observations—for instance, when zeolites are identified on volcanic glass samples formed more than 1 Ma ago.[49] These minerals precipitate according to the Ostwald rule of stages (glass → gel → smectites → zeolites) by progressive conversion of less stable minerals over geologic time at low

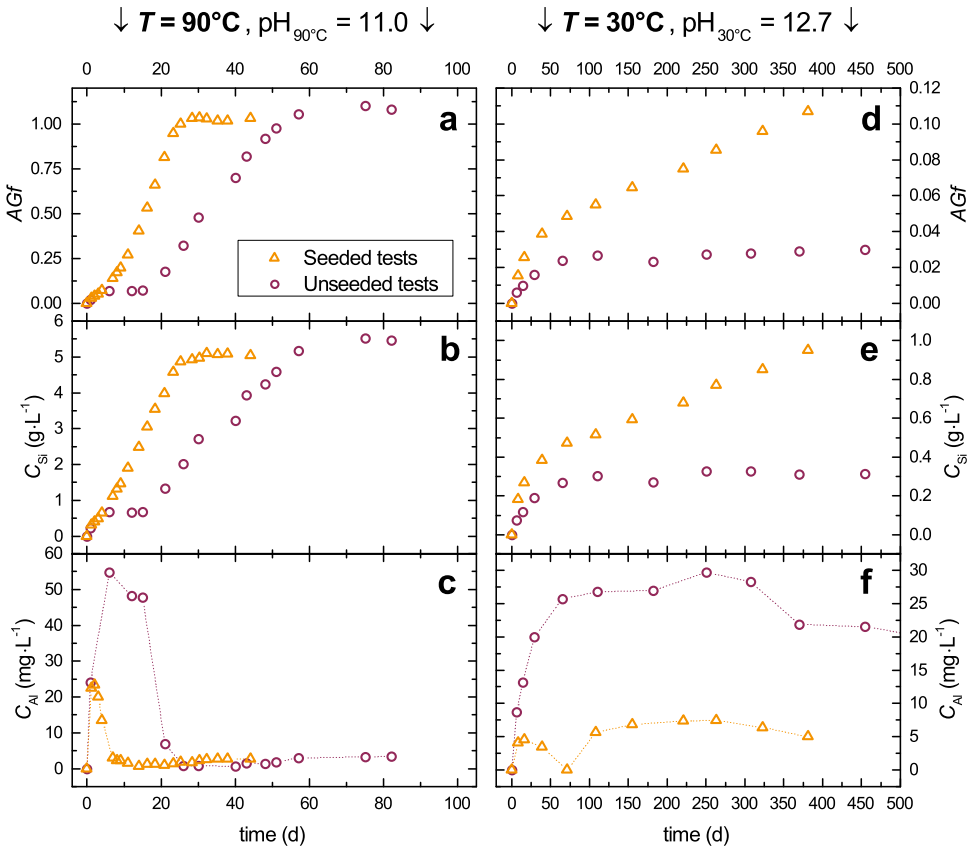

Fig. 8 Seeded vs. unseeded tests. Evolution over time of **a**, **d** the altered glass fraction AGf and of the concentrations of **b**, **e** silicon C_{Si} and **c**, **f** aluminum C_{Al} in tests carried out with $S/V = 1770\ m^{-1}$ and the same pOH at **a-c** 90 °C and **d-f** 30 °C, with or without seeding

temperature (e.g., close to 5 °C for Icelandic samples).

In Fig. 9a, at $pH_{90\,°C} = 10.4$, it appears that the glass alteration kinetics in the presence of seeds are faster, or at least equal, than those measured without seeding. The seeding impact is mainly visible during the latency period, between 30 and 120 days. Seed growth, initiated at the first instants, quickly consumes the aluminum available in solution, keeping its concentration at a low value (<1 mg L^{-1}). Zeolites precipitation competes with the formation of a potentially passivating layer on the glass surface. From 150 days, when the aluminum concentration becomes similar in both experiments, the alteration rates become equal, suggesting that the aluminum concentration—resulting from glass dissolution and zeolite precipitation kinetics—achieved a steady state.

At $pH_{90\,°C} = 10.1$ (Fig. 9b), the presence of seeds slightly accelerates the dissolution of the glass during the first 7 days before it stabilizes until Day 120. At this pH, seeding does not eliminate the latency period, which is, however, reduced and leads to the beginning of a RA after 120 days with a supposedly linear rate of 1.3×10^{-2} g m^{-2} d^{-1}. In the unseeded test, the drop in the aluminum concentration from Day 7 indicates resumption will likely occur soon. Thus, slow nucleation kinetics may explain why long latency periods can be observed prior to the occurrence of a resumption in environments for which thermodynamics indicates solution is saturated with respect to certain zeolites.

At "free" pH (Fig. 9c), there are no significant differences between seeded and unseeded tests: thus, there is no effect of the presence of Na-P2 zeolites on the occurrence of a resumption at $pH_{90\,°C} \approx 9$ (pH are given in Supplementary Fig. 9).

In these conditions, both solution analyses and SEM (Supplementary Fig. 10) show that the Na-P2 zeolite seeds do not significantly dissolve over the entire pH interval studied at 90 and 30 °C. This result differs from that of Ribet and Gin[9] showing the dissolution of neoformed merlinoite crystals during SON68 glass leaching in KOH solution after a pH decrease from 11.5 to 9 due to HCl addition. The stability of zeolites in a solution with respect to solubility strongly varies, depending on the nature of the mineral and the composition of the solution. At free pH, one hypothesis is that the solution is close to saturation with the seed phase.

Effect of pH and kinetic considerations

Both formation of a passivating layer and zeolite precipitation are dependent on pH and temperature conditions. The effects of these parameters on the RA are discussed in the following paragraphs. In the literature, laboratory tests demonstrating resumptions of alteration are associated with high pH: values above $pH_{90\,°C} = 11$ at 90 °C are generally cited.[6,50–52] These observations are confirmed in this study, showing a link between the pH and the resumption onset and rate. The ratios (i) between the initial rate and the resumption of the alteration rate (ii) and between the resumption of the alteration rate and the plateau rate are not constant. With the increase of pH, the resumption rate deviates from the plateau rate to approach—at an order of magnitude—the initial rate. Resumption rate is extremely sensitive to pH changes: e.g., it is multiplied by ≈60 with an increase in pH of approximately one unit (between $pH_{90\,°C} = 10.4$ and $pH_{90\,°C} = 11.3$).

Rates measured in different kinetics regimes are summarized in Fig. 10. It is shown that an effect of the presence of zeolites during ISG glass alteration in an alkaline environment (NaOH) is

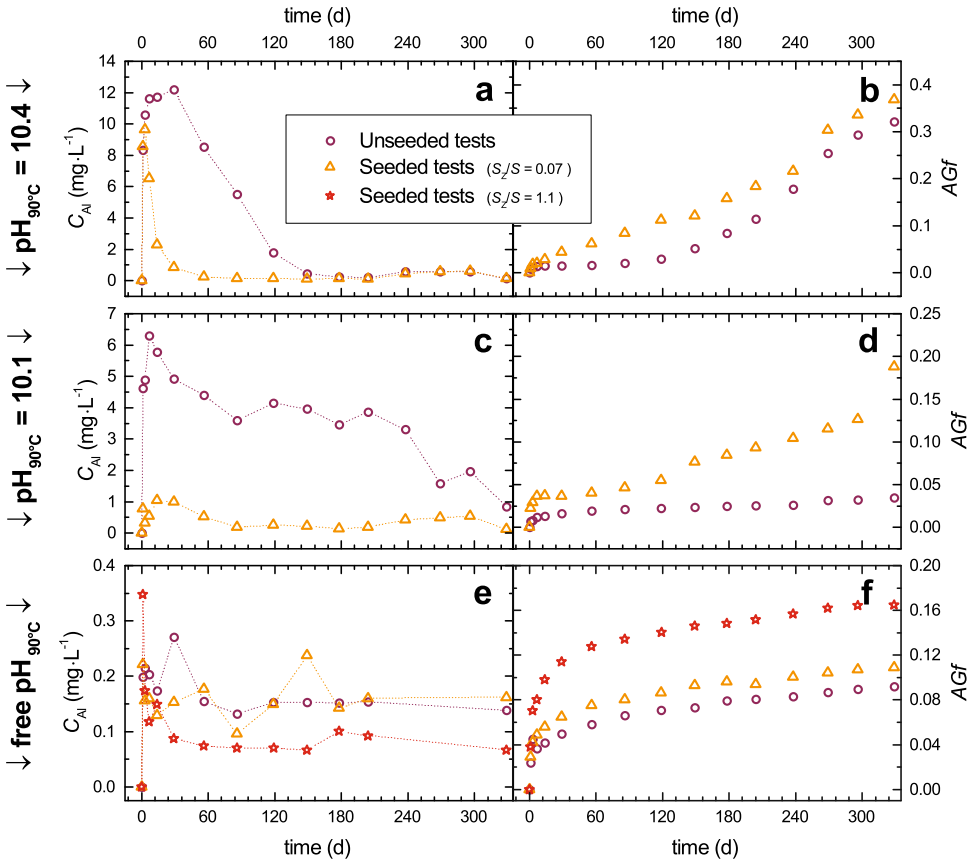

Fig. 9 Seeded vs. unseeded tests. Evolution over time of the aluminum concentration (C_{Al}) and the altered glass fraction (AGf) in tests carried out with $S/V = 1770\ m^{-1}$ at $pH_{90\,°C}$ = **a**, **b** 10.4, **c,d** 10.1 and **e,f** "free" pH ≈ 9

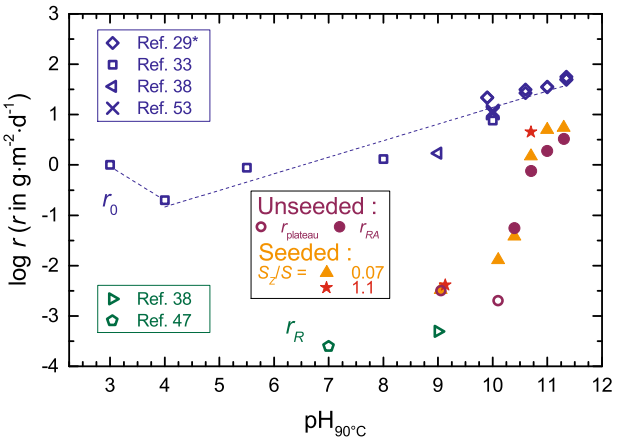

Fig. 10 Rates comparison. Maximum alteration rates measured at 90 °C in seeded and unseeded tests (given in Tables 1 and 2) compared with initial rates r_0[29,33,38,54] and residual rates r_R after 1 year.[38,47] Rates given at $pH_{90\,°C} = 9$ should decrease with time to the value from the literature.[38] *Initial rates were normalized according to Methods section

noticeable from $pH_{90\,°C} \approx 10.5$: the alteration rate then gradually approaches the initial rate r_0.

The alteration rates in seeded experiments are slightly higher than those reached in the absence of seeding: the growth of zeolites is therefore a driving force for the glass alteration. However, the initial rate remains the fastest alteration regime observed during the alteration of nuclear glasses.

Effect of temperature

The comparison of the results obtained at 30 and 90 °C, with the same pOH, confirms that the RA occurs earlier as the temperature increases.[52,53] These observations are consistent with the industrial synthesis of zeolites for which the rise in temperature reduces the latency period preceding crystal growth and accelerates the crystallization rate.

Moreover, the slowed down kinetics at 30 °C relative to 90 °C (Figs. 1b, 3b) make it possible to better appreciate that the decrease in aluminum concentration is a good indicator of the imminence of a RA. If no initial dissolution rate of ISG glass was measured at 30 °C, such rates can be extrapolated from the work of Inagaki, et al.[33] which provides data at 25 °C. At $pH_{30\,°C} = 13.1$, the extrapolated initial rate of $\approx 2 \times 10^{-3}\ g\ m^{-2}\ d^{-1}$ is greater by a factor of 100 than the resumption rate. For the same pOH, the ratio between the initial rate and the resumption of the alteration rate increases with the decrease in temperature.

Concluding remarks

- For ISG glass altered in an alkaline environment at 90 °C, results show the combined importance of pH and solution species that are nutrients for secondary phase nucleation and growth. Resumptions of alteration (stage 3) were observed from $pH_{90\,°C} = 10.1$. Their detrimental effects on glass durability decrease with decreasing pH. This is also the case at 30 °C.

- For borosilicate glasses with a typical Si/Al ratio much higher than that of zeolites, aluminum availability in solution is a key parameter for zeolite growth. Moreover, the decrease of

aluminum concentration—because of zeolite precipitation—is a good indicator of the shift towards a resumption regime, because it takes place before the increase of the boron concentration.
- Seeding is a useful tool to investigate long-term rates hardly accessible to laboratory measurements: it increases the glass alteration kinetics by reducing both the time taken to form stable nuclei and the kinetic limitation due to the lack of zeolite surface. Seeding thus enables the study of temperature–pH pairs relevant to nuclear waste disposal environments with laboratory tests.
- At pH ≈ 9 imposed by ISG glass dissolution in pure water at 90 °C, there are no significant consequences for glass durability of seeding by Na-P2 zeolites with seed surface area equal to that of glass.

According to the results presented in this study, it can be proposed that fast dissolution of ISG glass triggered by zeolites precipitation is not expected under near neutral and slightly basic pH conditions. The next step of this work will be to better quantify the relationship between zeolite surface and glass alteration kinetics in a tighter pH range between $pH_{90\,°C} = 9$ and 10. Moreover, it will be useful to define the formalism by which these results could improve glass alteration geochemical models; this will be performed in a future work.

METHODS

ISG glass preparation

ISG glass is a "simple" glass composed of six oxides (Supplementary Table 1) that are common to the vast majority of alumino-borosilicate nuclear glasses; their elemental ratios are the same as those of the French SON68 glass.[38] ISG glass production by MoSci Corporation (Rolla, Mo., United States) was described elsewhere.[10] ISG was chosen as an international reference glass for investigation of glass alteration, in order to provide for direct comparisons of test and modeling results from researchers worldwide.

Glass powder used in leaching tests is obtained by successive crushing steps with a planetary ball mill (Fritsch Pulverisette 5) and tungsten carbide grinding tools. Between each crushing step, powder is sieved to separate 63–125 µm and 125–250 µm size fractions. Powders are washed by an iterative process of sedimentation in acetone and absolute ethanol to remove fine particles.

Leaching tests

Leaching experiments consist of contacting ISG glass powder with sodium hydroxide solutions at different molarities. These experiments are performed in PFA (perfluoroalkoxy) reactors in static conditions. One of the major characteristics of these experiments is to maintain the pH at its initial value by regular additions of sodium hydroxide (±0.2 pH unit). At regular intervals, small volumes of solution are retrieved, filtered (cutoff: 10 kDa), acidified with ultrapure nitric acid and reserved at 7 °C for analysis. A powder sample may also be retrieved for additional analysis.

Leaching experiments are listed in Table 3. Test references are given according to the following formalism: name-$S/V(m^{-1})$-pH. Possible names are "S" for "seeded test" and "US" for "unseeded test". Uppercase letters are used for leaching tests at 90 °C and lowercase for those at 30 °C. The S_z/S parameter listed in the "Notes" column quantifies the amount of seeds as the ratio between the surface area of zeolite seeds and that of glass powder. Finally, a distinctive feature must be specified for the tests at $S/V = 70\ m^{-1}$: the small amount of glass compared to the volume of solution is insufficient to achieve a significant rate drop in silica free water within the duration of the experiment. Therefore, an initial amount of amorphous silica ($[Si]_0$) is dissolved in solution; this amount is determined from experiments at the higher S/V ratio.

The S/V ratio is calculated using the recommendations given by Fournier, et al.[54] The "reactive" surface area S is obtained by multiplying the geometric surface area S_{geo} of the glass powder samples—estimated by Eq. 1—by 1.3. In Eq. 1, ρ is the density of particles assimilated to spheres of average radius R_m.

$$S_{geo} = \frac{3}{\rho \times R_m} \quad (1)$$

Tests with an S/V ratio of 1770 m^{-1} were conducted with the 63–125 µm glass powder ($S_{geo} = 2.55 \times 10^{-2}\ m^2\ g^{-1}$; $S_{BET} = 7.20 \times 10^{-2}\ m^2\ g^{-1}$) and tests with an S/V ratio of 70 m^{-1} with the 125–250 µm glass powder ($S_{geo} = 1.28 \times 10^{-2}\ m^2\ g^{-1}$; $S_{BET} = 4.65 \times 10^{-2}\ m^2\ g^{-1}$).

The parameters whose effects are studied are (i) the S/V ratio (by comparing test series US-1770 and US-70 or test series S-1770 and S-70), (ii) the pH, (iii) seeding with zeolites (by comparing test series US and S or test series us and s), and the temperature (by comparing test series US and us or test series S and s).

Altered glass fraction

Inductively coupled plasma optical emission spectrometry (ICP-OES). Elemental concentrations in acidified solution samples were determined by ICP-OES (Thermo Scientific iCAP 6000 Series). In a sodium-rich medium, the quantification limits are 5, 20 and 20 µg L^{-1} for B, Al and Si, respectively. Elemental concentrations in the starting solutions were below the detection limits, except for Na (used to adjust pH) and K (as traces in sodium hydroxide solution and released by pH electrode). Note that Ca analyses give inconsistent results, and Zr concentration is consistently below the quantification limit.

Calculation of the AGf. The iterative calculation of the AGf could be performed from solution concentrations of glass components released during glass leaching. Such calculation considers the variations in volume due to samplings, solution additions or evaporation, according to Eq. 2, where $C_i(t)$ is the concentration of element i in solution at time t, x_i is its mass fraction in glass, $V(t)$ is the volume of solution, $V_s(j)$ is the volume of the jth sampling, and m is the mass of glass powder. Equation 2 expressed an AGf only if element i is not retained in the amorphous layer or in the secondary precipitated phases. Boron, known to be a good glass alteration tracer, is chosen for AGf calculations.

$$\mathrm{AGf} = \frac{C_i(t) \times V(t) + \sum_{j=1}^{t-1} C_i(j) \times V_s(j)}{m \times x_i} \quad (2)$$

From Eq. 2 is deduced the equivalent thicknesses of altered glass eTh_i—or the normalized mass loss NL_i—according to Eq. 3 . The glass alteration rate is then equal to $dNL_i/dt \propto deTh_i/dt$.

$$eTh_i = \frac{NL_i}{\rho} = R_m \times \left(1 - \sqrt[3]{1 - \mathrm{AGf}}\right) \quad (3)$$

Zeolite seeds synthesis

Zeolites Na-P are of interest in this study and should be used as seeds. Thus, a synthesis protocol of such zeolite seeds derived from those proposed by Regis et al.[55] and Taylor and Roy[46] was developed. Seeds were obtained by mixing sources of sodium (sodium hydroxide), aluminum (sodium aluminate) and silicon (amorphous silica) in ultrapure water with the stoichiometry 6 Na_2O:1 Al_2O_3:8 SiO_2 and a liquid/solid ratio of 6/1 wt/wt.

The synthesis proceeds according to the following steps.

i. Sodium hydroxide is dissolved in the total volume of ultrapure water (18 MΩ·cm). After dissolution, the solution obtained is divided into two fractions (¾:¼).
ii. The first fraction of the sodium hydroxide solution (¾ of the total volume) is used for dissolving amorphous silica under stirring at 90 °C for approximately 1 week.
iii. The remaining fraction of sodium hydroxide solution (¼ of the total volume) allows the dissolution of the sodium aluminate in a few minutes at room temperature.
iv. Solutions prepared at steps (ii) and (iii) are mixed in a PFA reactor under vigorous stirring until formation of a homogeneous gel. The mixture is then placed in an oven at 100 °C for 7 days without stirring.
v. At the end of the 7 day period, the reactor contains a mixture of zeolites and coarse material. To collect pure zeolite crystals, the contents of the reactor are put into ultrapure water and stirred for a few seconds. After stirring is stopped and when the coarse material

Table 3. Leaching tests conducted with ISG glass

Test reference[a]	T (°C)	S/V (m^{-1})	pH_T[b]	pOH	$[Na^+]_0$ (mM)	Notes
US-1770-11.3	90	1 770	11.3	0.8	250	
US-1770-11.0	90	1 770	11.0	1.1	79	
US-1770-10.7	90	1 770	10.7	1.4	25	
US-1770-10.4	90	1 770	10.4	1.7	10.3	
US-1770-10.1	90	1 770	10.1	2.0	5.0	
US-1770-F	90	1 770	free[c]		0	
US-70-11.3	90	70	11.3	0.8	250	$[Si]_0 = 92$ mM[d]
US-70-11.0	90	70	11.0	1.1	79	$[Si]_0 = 23$ mM[d]
US-70-10.7	90	70	10.7	1.4	25	$[Si]_0 = 10$ mM[d]
us-1770-13.1	30	1 770	13.1	0.8	250	$pH_{30\,°C}$ 13.1 ~ $pH_{90\,°C}$ 11.3
us-1770-12.7	30	1 770	12.7	1.1	79	$pH_{30\,°C}$ 12.7 ~ $pH_{90\,°C}$ 11.0
us-1770-12.3	30	1 770	12.3	1.4	25	$pH_{30\,°C}$ 12.3 ~ $pH_{90\,°C}$ 10.7
S-1770-11.3	90	1 770	11.3	0.8	250	$S_z/S = 0.07$[e]
S-1770-11.0	90	1 770	11.0	1.1	79	$S_z/S = 0.07$[e]
S-1770-10.7	90	1 770	10.7	1.4	25	$S_z/S = 0.07$ to 1.1[e,f]
S-1770-10.4	90	1 770	10.4	1.7	10.3	$S_z/S = 0.07$[e]
S-1770-10.1	90	1 770	10.1	2.0	5.0	$S_z/S = 0.07$[e]
S-1770-F	90	1 770	free[c]		0	$S_z/S = 0.07$ and 1.1[e,f]
S-70-11.3	90	70	11.3	0.8	250	$[Si]_0 = 92$ mM[d]. $S_z/S = 1.5$[e]
S-70-11.0	90	70	11.0	1.1	79	$[Si]_0 = 23$ mM[d]. $S_z/S = 1.5$[e]
S-70-10.7	90	70	10.7	1.4	25	$[Si]_0 = 10$ mM[d]. $S_z/S = 1.5$[e]
s-1770-13.1	30	1 770	13.1	0.8	250	$S_z/S = 0.07$[e]. $pH_{30\,°C}$ 13.1 ~ $pH_{90\,°C}$ 11.3
s-1770-12.7	30	1 770	12.7	1.1	79	$S_z/S = 0.07$[e]. $pH_{30\,°C}$ 12.7 ~ $pH_{90\,°C}$ 11.0
s-1770-12.3	30	1 770	12.3	1.4	25	$S_z/S = 0.07$[e]. $pH_{30\,°C}$ 12.3 ~ $pH_{90\,°C}$ 10.7

[a] Test references are given according to the following formalism: name-S/V(m^{-1})-pH. Possible names are "US" for "unseeded test" and "S" for "seeded test". Uppercase letters are used for leaching tests at 90 °C and lowercase for those at 30 °C
[b] pH is given at the test temperature (90 or 30 °C)
[c] "Free pH" tests are conducted in initially pure water, and the pH is allowed to drift freely
[d] With an S/V ratio of 70 m^{-1}, reaching the rate drop would require a greater amount of silicon than that contained in the glass. That is why an initial amount of silicon $[Si]_0$ is added to the solution
[e] The S_z/S parameter quantifies the seeding level as the ratio between the surface area of zeolite seeds initially added to the test and that of glass powder
[f] Seeded tests with several amounts of seeds
The table indicates successively the test reference, the temperature at which the test is conducted, its S/V ratio, the pH (or pOH calculated with $pK_w = 12.1$ at 90 °C) maintained throughout the test, the initial sodium concentration in solution, and any test distinctive features

settles, the first one-third of the suspension is filtered in a Büchner funnel. This operation is repeated until the first third of the suspension is clear. The product obtained is rinsed and dried.

Solid analysis

Gas sorption. Specific surfaces (S_{BET}) of glass and seed samples were measured by adsorption of krypton on the sample surface (Micromeritics ASAP 2020). The samples were degassed at 200 °C under a vacuum of at least 0.13 Pa. The amount of gas required to form a monoatomic layer on the surface of the sample was estimated by the Brunauer–Emmett–Teller theory.[56]

Thermogravimetric analysis (TGA). The water content of zeolite seeds was determined by TGA (SETARAM G70 thermoanalyzer) from 100 mg of sample placed in a Pt-Au crucible (8 mm in diameter, 2 cm in height) and heated in an air atmosphere type electrical furnace with a temperature increase to 1000 °C, followed by cooling to room temperature.

Infrared (IR) spectroscopy. IR spectra were collected on a Fourier transform IR spectrometer-attenuated total reflectance (Bruker Vertex 70) equipped with a DTGS-KBr detector. The zeolite seed sample was placed on the surface of the diamond and pressed with a piston. Spectrums were recorded between 400 and 4000 cm^{-1}, accumulating 32 acquisitions of 4 s, and processed using OPUS software (Bruker).

Laser diffraction. Laser diffraction (Malvern Mastersizer 3000) was used to calculate seeds size distribution using the Mie theory and assuming a volume equivalent sphere model. Refractive indexes were taken equal to 1.48 for the seeds and 1.33 for the dispersant (water). The results were divided into 100 size fractions logarithmically distributed between 10^{-2} and 3×10^3 µm to determine the particle size distribution.

X-ray diffraction (XRD). XRD patterns were acquired with a Phillips X'PERT Pro equipped with a Bragg–Brentano θ–2θ diffractometer and operated with monochromatic Cu-Kα_1 radiation (1.5418 Å) at 40 mA–40 kV. Acquisitions were performed on the 2θ range extending from 4° to 80° with a speed of 0.11° min^{-1} and a step of 0.017° (2θ). Data were processed by DIFFRAC.EVA software (Bruker) and compared with reference diffractograms of the ICDD PDF-4+ (2015) database.

Scanning electron microscopy (SEM). Field emission SEM observations were made with a Zeiss SUPRA 55, operated with a 15 kV acceleration voltage, equipped with detectors of secondary and backscattered electrons and coupled with a lithium-drifted silicon detector for elemental analysis by energy dispersive X-ray spectroscopy (EDS). Cross sections were prepared by coating samples in an epoxy resin and polishing with SiC abrasive papers and with cloths and diamond suspensions (final polishing: 1 µm) before metallization by deposition of carbon.

Data availability

The authors declare that the data supporting the findings of this study are available within the article and its supplementary information files, and from the corresponding author upon reasonable request.

ACKNOWLEDGEMENTS

The authors are very grateful to Elodie Nicoleau, Marc Samman, Aurélien Ull, Jean-Pierre Mestre, Nicolas Massoni and Pascal Antonucci for their active participation in the success of the experiments and for their valuable advice. This work was funded by the French Alternative Energies and Atomic Energy Commission (CEA) and AREVA.

AUTHOR CONTRIBUTIONS

M.F. performed the experiments and wrote the paper. S.G. and P.F. supervised the study. S.G., P.F. and S.M.-D. were deeply involved in the interpretation of the data and the paper reviews.

ADDITIONAL INFORMATION

Supplementary information accompanies the paper on the *npj Materials Degradation* website (https://doi.org/10.1038/s41529-017-0018-x).

Competing interests: The authors declare that they have no competing financial interests.

Publisher's note: Springer Nature remains neutral with regard to jurisdictional claims in published maps and institutional affiliations.

REFERENCES

1. Vienna, J. D., Ryan, J. V., Gin, S. & Inagaki, Y. Current understanding and remaining challenges in modeling long-term degradation of borosilicate nuclear waste glasses. *Int. J. Appl. Glass Sci.* **4**, 283–294 (2013).
2. Fournier, M., Gin, S. & Frugier, P. Resumption of nuclear glass alteration: state of the art. *J. Nucl. Mater.* **448**, 348–363 (2014).
3. Mercado-Depierre, S., Fournier, M., Gin, S. & Angeli, F. Influence of zeolite precipitation on borosilicate glass alteration under hyperalkaline conditions. *J. Nucl. Mater.* **491**, 67–82 (2017).
4. Ebert, W. L. & Bates, J. K. A comparison of glass reaction at high and low glass surface/solution volume. *Nucl. Technol.* **104**, 372–384 (1993).
5. Barkatt, A., Macedo, P. B., Gibson, B. C. & Montrose, C. J. Modelling of waste performance and system release. *Mater. Res. Soc. Symp. Proc.* **44**, 3–13 (1985).
6. Feng, X. D., Bates, J. K., Buck, E. C., Bradley, C. R. & Gong, M. L. Long-term comparison of dissolution behavior between fully radioactive and simulated nuclear waste glasses. *Nucl. Technol.* **104**, 193–206 (1993).
7. Muller, I. S. Renewal of corrosion progress after long term leaching. in *Summer Session Proceedings on Glass: Scientific Research for High Performance Containment*, 269–274 (CEA/Valrhô, Méjannes-Le-Clap, France 1997).
8. Ebert, W. L., Bakel, A. J. & Brown, N. R. Measurement of the glass dissolution rate in the presence of alteration phases. in *Proceedings of International Conference Nuclear and Hazardous Waste Management, Spectrum'96* 453–460 (American Nuclear Society, La Grange Park, US 1996).
9. Ribet, S. & Gin, S. Role of neoformed phases on the mechanisms controlling the resumption of SON68 glass alteration in alkaline media. *J. Nucl. Mater.* **324**, 152–164 (2004).
10. Gin, S. et al. The fate of silicon during glass corrosion under alkaline conditions: a mechanistic and kinetic study with the international simple glass. *Geochim. Cosmochim. Acta* **151**, 68–85 (2015).
11. ANDRA. *Dossier 2005 Argile: Tome Phenomenological evolution of a geological repository* (2006). https://www.andra.fr/download/andra-international-en/document/editions/269va.pdf.
12. Mochida, I. et al. The effects of seeding in the synthesis of zeolite MCM-22 in the presence of hexamethyleneimine. *Zeolites* **18**, 142–151 (1997).
13. Thompson, R. in *Molecular Sieves* (Karge, H. G., Weitkamp J. eds) Vol. 1, Ch. 1, 1–33 (Springer, Berlin, Heidelberg, 1998).
14. Rees, C. A., Provis, J. L., Lukey, G. C. & van Deventer, J. S. J. The mechanism of geopolymer gel formation investigated through seeded nucleation. *Colloids Surf. A* **318**, 97–105 (2008).
15. Majano, G., Darwiche, A., Mintova, S. & Valtchev, V. Seed-induced crystallization of nanosized Na-ZSM-5 Crystals. *Ind. Eng. Chem. Res.* **48**, 7084–7091 (2009).
16. Kamimura, Y., Itabashi, K. & Okubo, T. Seed-assisted, OSDA-free synthesis of MTW-type zeolite and "Green MTW" from sodium aluminosilicate gel systems. *Microporous Mesoporous Mater.* **147**, 149–156 (2012).
17. Kamimura, Y. et al. OSDA-free synthesis of MTW-type zeolite from sodium aluminosilicate gels with zeolite beta seeds. *Microporous Mesoporous Mater.* **163**, 282–290 (2012).
18. Kamimura, Y. et al. Crystallization behavior of zeolite Beta in OSDA-Free, seed-assisted synthesis. *J. Phys. Chem. C* **115**, 744–750 (2010).
19. Wu, Z., Song, J., Ji, Y., Ren, L. & Xiao, F.-S. Organic template-free synthesis of ZSM-34 zeolite from an assistance of zeolite L seeds solution. *Chem. Mater.* **20**, 357–359 (2007).
20. Zhang, H. et al. Organotemplate-free synthesis of high-silica ferrierite zeolite induced by CDO-structure zeolite building units. *J. Mater. Chem.* **21**, 9494–9497 (2011).
21. Xie, B. et al. Seed-directed synthesis of zeolites with enhanced performance in the absence of organic templates. *Chem. Commun.* **47**, 3945–3947 (2011).
22. Xie, B. et al. Organotemplate-free and fast route for synthesizing beta zeolite. *Chem. Mater.* **20**, 4533–4535 (2008).
23. Diaz, U., Fornes, V. & Corma, A. On the mechanism of zeolite growing: crystallization by seeding with delayered zeolites. *Microporous Mesoporous Mater.* **90**, 73–80 (2006).
24. Bates, J. K., Seintz, M. G. & Steindler, M. J. The relevance of vapor phase hydration aging to nuclear waste isolation. *Nucl. Chem. Waste Manage* **5**, 63–73 (1984).
25. Neeway, J. et al. Vapor hydration of SON68 glass from 90°C to 200°C: a kinetic study and corrosion products investigation. *J. Non Cryst. Solids* **358**, 2894–2905 (2012).
26. Wronkiewicz, D. J. & Arbesman, K. A. The role of alteration phases in influencing the kinetics of glass dissolution. *Mater. Res. Soc. Symp. Proc.* **608**, 745–750 (1999).
27. Gauthier, A., Thomassin, J.-H. & Le Coustumer, P. Rôle de matériaux zéolitiques lors de l'altération expérimentale du verre nucléaire R7T7. *C.R. Acad. Sci. Ser. IIA* **329**, 331–336 (1999).
28. Fournier, M., Frugier, P. & Gin, S. Effect of zeolite formation on borosilicate glass dissolution kinetics. *Procedia Earth Planet. Sci.* **7**, 264–267 (2013).
29. Fournier, M., Frugier, P. & Gin, S. Resumption of alteration at high temperature and pH: rates measurements and comparison with initial rates. *Procedia Mater. Sci* **7**, 202–208 (2014).
30. Gin, S. et al. The controversial role of inter-diffusion in glass alteration. *Chem. Geol.* **440**, 115–123 (2016).
31. Gin, S. et al. Atom-probe tomography, TEM and ToF-SIMS study of borosilicate glass alteration rim: a multiscale approach to investigating rate-limiting mechanisms. *Geochim. Cosmochim. Acta* **202**, 57–76 (2017).
32. Chave, T., Frugier, P., Ayral, A. & Gin, S. Solid state diffusion during nuclear glass residual alteration in solution. *J. Nucl. Mater.* **362**, 466–473 (2007).
33. Inagaki, Y., Kikunaga, T., Idemitsu, K. & Arima, T. Initial dissolution rate of the International Simple Glass as a function of pH and temperature measured using microchannel flow-through test method. *Int. J. Appl. Glass Sci.* **4**, 317–327 (2013).
34. Donahoe, R. J. & Liou, J. G. An experimental study on the process of zeolite formation. *Geochim. Cosmochim. Acta* **49**, 2349–2360 (1985).
35. Lechert, H. The pH value and its importance for the crystallization of zeolites. *Microporous Mesoporous Mater.* **22**, 521–523 (1998).
36. Houston, J. R., Maxwell, R. S. & Carroll, S. A. Transformation of meta-stable calcium silicate hydrates to tobermorite: reaction kinetics and molecular structure from XRD and NMR spectroscopy. *Geochem. Trans.* **10** (2009).
37. Kohoutkova, M., Klouzkova, A., Maixner, J. & Mrazova, M. Preparation and characterization of analcime powders by X-ray and SEM analyses. *Ceram. Silik.* **51**, 9–14 (2007).
38. Gin, S., Beaudoux, X., Angéli, F., Jégou, C. & Godon, N. Effect of composition on the short-term and long-term dissolution rates of ten borosilicate glasses of increasing complexity from 3 to 30 oxides. *J. Non Cryst. Solids* **358**, 2559–2570 (2012).
39. Milton, R. M. Crystalline zeolite B (1961). Patent issuing from United States Patent Office (Patent version number: 3,008,803).
40. Gatta, G. D., Lotti, P., Nestola, F. & Pasqual, D. On the high-pressure behavior of gobbinsite, the natural counterpart of the synthetic zeolite Na-P2. *Microporous Mesoporous Mater.* **163**, 259–269 (2012).
41. Hansen, S., Hakansson, U. & Falth, L. Structure of synthetic zeolite Na-P2. *Acta Crystallogr. C Struct. Chem.* **46**, 1361–1362 (1990).
42. Flanigen, E. M., Khatami, H. & Szymanski, H. A. in *Advances in Chemistry* (Edith M. Flanigen, Leonard B. Sand eds) Vol. 101, Ch. 16, 201–229 (American Chemical Society, Washington, US 1974).
43. Breck, D. W. *Zeolite Molecular Sieves: Structure, Chemistry, and Use* (Wiley, New York, US, 1973).
44. Huo, Z. et al. Synthesis of zeolite NaP with controllable morphologies. *Microporous Mesoporous Mater.* **158**, 137–140 (2012).

45. Barrer, R. M. & Munday, B. M. Cation exchange reactions of zeolite Na-P. *J. Chem. Soc. A Inorg. Phys. Theor*. 2909–2914 (1971).
46. Taylor, A. M. & Roy, R. Zeolite studies IV: Na-P zeolites and the ion-exchanged derivatives of tetragonal Na-P. *Am. Mineral.* **49**, 656–682 (1964).
47. Gin, S. et al. Origin and consequences of silicate glass passivation by surface layers. *Nat. Commun*. **6**, 6360 (2015).
48. Rajmohan, N., Frugier, P. & Gin, S. Composition effects on synthetic glass alteration mechanisms: Part 1. Experiments. *Chem. Geol.* **279**, 106–119 (2010).
49. Crovisier, J. L., Advocat, T. & Dussossoy, J. L. Nature and role of natural alteration gels formed on the surface of ancient volcanic glasses (Natural analogs of waste containment glasses). *J. Nucl. Mater.* **321**, 91–109 (2003).
50. Gin, S. & Mestre, J. P. SON 68 nuclear glass alteration kinetics between pH 7 and pH 11.5. *J. Nucl. Mater.* **295**, 83–96 (2001).
51. Ribet, S., Muller, I. S., Pegg, I. L., Gin, S. & Frugier, P. Compositional effects on the long-term durability of nuclear waste glasses: a statistical approach. *Mater. Res. Soc. Symp. Proc.* **824**, 309–314 (2004).
52. Inagaki, Y. et al. Aqueous alteration of Japanese simulated waste glass P0798: effects of alteration-phase formation on alteration rate and cesium retention. *J. Nucl. Mater.* **354**, 171–184 (2006).
53. Gan, X. Y. et al. Long-term product consistency test of simulated 90-19/Nd HLW glass. *J. Nucl. Mater.* **408**, 102–109 (2011).
54. Fournier, M. et al. Glass dissolution rate measurement and calculation revisited. *J. Nucl. Mater.* **476**, 140–154 (2016).
55. Regis, A. J., Sand, L. B., Calmon, C. & Gilwood, M. E. Phase studies in the portion of the soda-alumina-silica water system producing zeolites. *J. Phys. Chem.* **64**, 1567–1571 (1960).
56. Brunauer, S., Emmett, P. H. & Teller, E. Adsorption of gases in multimolecular layers. *J. Am. Chem. Soc.* **60**, 309–319 (1938).